Equilibrium spherically curved two-dimensional Lennard-Jones systems

J. M. Voogd[a] and P. M. A. Sloot
University of Amsterdam, Section Computational Science, Kruislaan 403, 1098 SJ Amsterdam, The Netherlands

R. van Dantzig[b]
National Institute for Nuclear Physics and High Energy Physics (NIKHEF), Kruislaan 409, 1098 SJ Amsterdam, The Netherlands

(Received 26 April 2005; accepted 30 June 2005; published online 30 August 2005)

To learn about the basic aspects of nanoscale spherical molecular shells during their formation, spherically curved two-dimensional N-particle Lennard-Jones systems are simulated, studying curvature evolution paths at zero temperature. For many N values ($N<800$) equilibrium configurations are traced as a function of the curvature radius R. Sharp jumps for tiny changes in R between trajectories with major differences in topological structure correspond to avalanche-like transitions. For a typical case, $N=25$, equilibrium configurations fall on smooth trajectories in state space which can be traced in the E-R plane. The trajectories show up with local energy minima, from which growth in N at steady curvature can develop. © *2005 American Institute of Physics*. [DOI: 10.1063/1.2007707]

I. INTRODUCTION

In vitro self-organization in aqueous solution of nanoscale spherical shells, like various types of nanovesicles[1–4] and viral capsids,[5] is a thermodynamic process driven by overall free-energy minimization. The resulting shell has inherent tendencies towards (a) crystalline structure,[6–8] (b) global polyhedral symmetry,[9–11] and (c) discrete sizes,[1,12,13] thus discrete curvatures.

A compelling question is whether during the thermodynamic growth a transient uncompleted (open) shell of a given N prefers intrinsically to adopt a specific equilibrium radius of curvature (R), and whether this radius—on the basis of molecular packing order already—may be approximately stable during (part of) that growth. The occurrence of local minima in the mean (per particle) potential energy (E) of an emerging shell as a function of all internal degrees of freedom—including R—along the evolution path in state space, could thus be significant for steady curvature during the growth in N.

In this paper we approach the problem in a much simplified model that allows systematic generic studies. The sphericity of the shell, in reality due to intrinsic 3D properties of the optimally closely packed molecular subunits, is built-in as a global geometrical constraint. We perform computer experiments with freely relaxing—possibly open—spherically curved zero-thickness monolayers of identical molecules, studying the structural properties in relation with N and R. Our approach is most natural for monolayer nanowheel vesicles,[4] but it is as well relevant for tiny bilayer vesicles, where the laterally most densely packed pseudocrystalline inner lipid head group sublayer can act as monolayer "backbone."

As model we use two-dimensional (2D) Lennard-Jones (LJ) N-particle systems on a spherical surface with flexible radius at zero temperature.[6,14] The LJ potential $V_{ij}=r_{ij}^{-12}-2r_{ij}^{-6}$ between two particles i and j with Euclidean distance r_{ij} energetically favors close regular packing with essentially unit distance between neighboring particles.[6] The LJ form in the constrained system acts as an effective interaction mimicking the real complex of interactions. It allows a comprehensive systematic exploration while keeping salient features of real systems. The present work arises from a series of computational studies[6] on 2D spherical crystallization in LJ systems over a broad range of N, involving thermodynamic behavior and zero-temperature global energy minimization. The LJ systems follow local equilibrium paths in state space, realistically allowing for local minimum "hang ups" in evolving configurations.

When many LJ particles are randomly spread over a flat surface they aggregate into an approximately homogeneous configuration, a major fraction of the particles being trapped inside the bulk (interior). Edge particles have higher energy than bulk particles, giving rise to edge tension, the 2D equivalent of surface tension. Minimizing edge energy, flat aggregates become approximately circular patches. Minimizing the overall potential energy, the bulk becomes an essentially regular hexagonal lattice. Allowing for spherical curvature, the 2D system can further decrease the energy by reducing the edge length and by a rising attraction from LJ tails of remote particles (the LJ forces acting in 3D). This energy gain by curvature, however, balances against increasing strain energy of the bulk because of less favorable packing.

Our question becomes whether—thanks to the interplay

[a]Present address: TNO-FEL, NL-2597AK The Haque, The Netherlands.
[b]Author to whom correspondence should be addressed. Electronic mail: rvd@nikhef.nl

of these R-dependent nonlinear effects—equilibrium radii R_{eq} can be found where relaxation after any small change in curvature raises E, and freely variable R leads the system back to the same equilibrium radius. If such local energy minima in *open* configurations are thermodynamically significant, they can stabilize transient states along a path of growing N. This is supported by a LJ study,[15] showing that *closed* global minimum energy N-particle configurations (covering the whole sphere) strongly correlate with specific *open* local minimum configurations of lower N.

II. METHODS

In our experiments, each time the radius R is changed by a small step, the particle system is relaxed by minimizing—at the new R value—the mean energy, which implies reaching the nearest equilibrium configuration. The system is thus evolved in curvature, while staying in equilibrium with changing R. For *relaxation* (equilibration of forces and energy minimization), a steepest descent (SD) algorithm[16] is applied while for *aggregation* a Metropolis Monte Carlo simulated annealing[17] (SA) optimization is used. The latter method enhances the probability that the system ends up in a *global* energy minimum[18] (GEM) rather than in a local secondary energy minimum. The 2D topology of a configuration is defined by the Voronoi nearest-neighbors method,[19] giving each particle a coordination number (CN), which is 6 everywhere for a flat (hexagonal) GEM configuration. The value CN–6 is denoted as the disclination charge—short d charge—of a particle. In a 2D topological structure any single built-in defect—disclination or dislocation (tightly bound pair of disclinations with opposite d charge)—can be displaced but not removed, except by its annihilation as part of a set of converging complementary defects or by moving it all the way to the edge. During the transformation of a flat GEM lattice to a closed shell a net total d charge of -12 must be incorporated in the full Voronoi lattice. In addition, dislocations have the function of lowering the strain energy in total, by distributing it locally more evenly.[6]

How much the configurations change during relaxation after a step ΔR can be expressed as the mean Euclidean distance $\hat{r}$ traveled between the associated sets of coordinates $\mathbf{x}_R$ and $\mathbf{x}_{R+\Delta R}$ in configuration space (mean taken per particle and per percent change in curvature),

$$\hat{r} = (|\Delta R|/RN) \sqrt{\sum_{i=1}^{N} (\mathbf{x}_{R,i} - \mathbf{x}_{R+\Delta R,i})^2}.$$

III. COMPUTER EXPERIMENTS

A. From flat to spherical

In the first series of experiment we explore gross changes in the topological and geometrical structures and the corresponding energy with monotonously decreasing R. For hundreds of runs with $N<800$ an initial, circularlike aggregate is prepared from a flat regular hexagonal lattice with unit spacing (GEM for infinite N in flat 2D). In the experiments R is decreased in 1% steps, each time the configuration is being projected onto the new sphere and then relaxed using the SD method. The decrease in R is continued until the system is compressed considerably. A system of particular N follows a "standard" (for that N) evolution path through state space and through the E-R plane.

B. Example, $N=25$

Curved lattices unbiased by any initial configuration and path history are simulated while starting in SA mode at high temperatures ($T=10$) in a random configuration and then aggregated by cooling down the system in 5% $\Delta T/T$ steps. SD is applied as final tuning. This study is done for a *typical* "*unmagic*" N value, $N=25$. In 1300 runs radii are randomly chosen between $R=1.3$ and $R=2$.

The equilibrium points in E-R space align over a range of R values along distinct smooth trajectories: lines which correspond to continuous sets of topologically and geometrically closely similar equilibrium configurations.

C. Tracing up and down in curvature

The central question of the current paper, whether trajectories of the system lining up closely related configurations can provide a stable system against a freely variable R, is addressed in a third type of experiment. Starting from particular open $N=25$ configurations obtained in the second experiment, trajectories are traced (with relaxation) step by step in R in both directions, and the structure is investigated.

IV. RESULTS AND DISCUSSION

A. Energy trends

In the first study a general energy trend is found for all N values, as illustrated by three typical examples: for $N=6$, 50, and 350 in Fig. 1 (left column). As expected, the most prominent feature is a deep *global* minimum along the followed E-R path. Having started from a flat regular configuration while systematically decreasing R, the particles cover in close packing an increasing part of the sphere until at the closure radius R_c, the lowest E along the E-R path is reached. At this stage any uncovered area—and thus any edge—has disappeared. We note that, except for details, the structure is not biased significantly by the initial configuration.

The energy difference ΔE_c between the $R\to\infty$ asymptotic value and the deep minimum represents the energy gain of closure. Additional structures are visible: secondary, local, minima and sharp downward jumps at $R>R_c$.

Towards smaller radii $R<R_c$, the system comes under an external pressure and the density increases. The LJ repulsive core between neighboring particles then increasingly dominates the energy, the energy rises steeply, independent of the detailed configuration.

The energy of a configuration can be approximated as $E=(N_{bulk}\epsilon_{bulk}+N_{edge}\epsilon_{edge})/N$, where $N_{bulk}+N_{edge}=N$, $\epsilon_{bulk}=-3.382$ being the lowest possible value corresponding to an infinite flat regular hexagonal lattice, while ϵ_{edge} is typically half of that value. Due to the impossibility of a fully regular hexagonal packing, ϵ_{bulk} is higher on a curved surface. The unfavorable edge energy forms the main driving force for

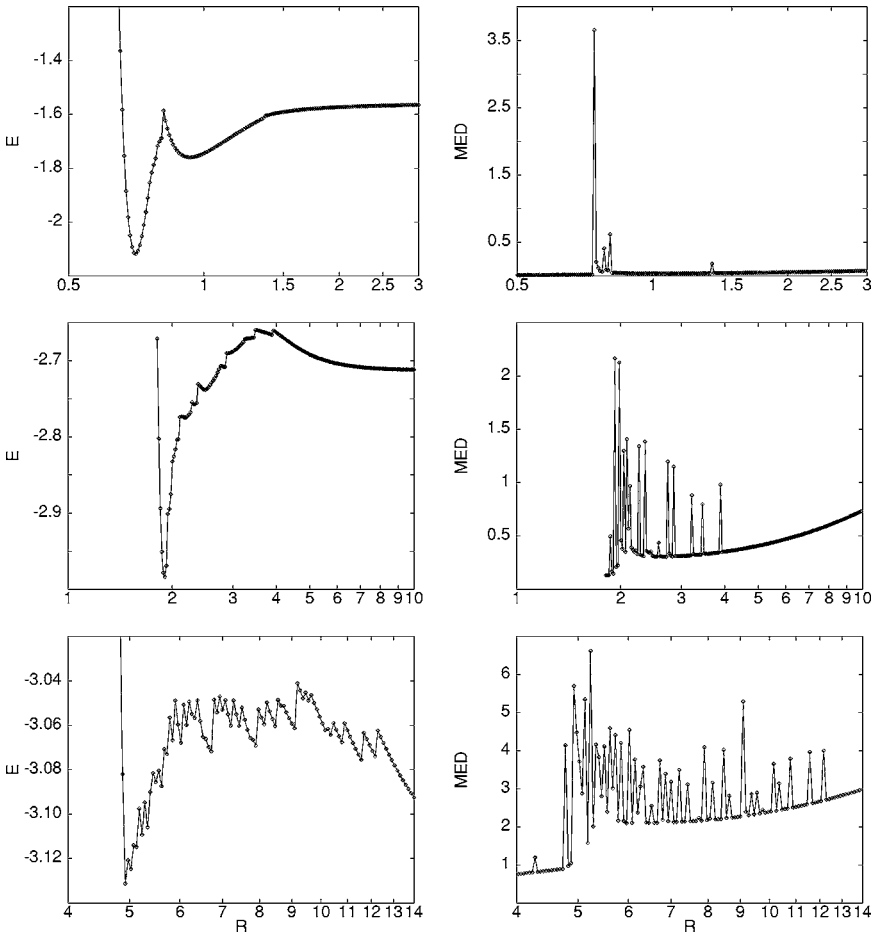

FIG. 1. Data from the first series of experiments: from top to bottom for $N=6$, 50, and 350 the mean potential energy (E) (at left), and the mean Euclidean distance (MED, $\hat{r}$) traveled in configuration space during equilibration after 1% downward steps in curvature radius (R). The system was initiated in a flat regular configuration.

curvature and shell closure, although—due to the topological rearrangement—normally a barrier between the flat and curved states stands in the way. Consequently, for the larger N values, starting from the flat GEM configuration, indeed dE/dR is negative, meaning that at sufficiently low T such a flat LJ system is locally stable against curvature. An exception is the extreme case, $N=6$, where the initially flat LJ system can immediately gain energy by curving. A tiny jump in E (at $R\approx 1.36$) goes with a discontinuity in the dE/dR slope. Here already we observe a secondary minimum along the standard E-R path. For $N=50$ below $R=4$, the local energy minima and jumps are visible. At $R_c\approx 1.87$ the system closes over the sphere. For $N=350$ below $R=13$, many minima and many jumps show up. At $R_c\approx 5$ the system closes. In the second experiment ($N=25$), in Fig. 2(a), the independently obtained E values for fixed, randomly chosen, R values align along smooth lines in the E-R plane.

B. Euclidean distance

Energy jumps (Fig. 1 at left) go with structural transitions visible as spikes in the mean Euclidean distance per particle per percent, $\hat{r}(R)$ (Fig. 1 at right). At $R<R_c$, the particles hardly move anymore over the sphere, all flexibility being lost due to the external pressure counterbalanced by the repulsive core. The smooth background in $\hat{r}(R)$ reflects small adjustments of an essentially stable configuration after a curvature step. It can be fully suppressed by reducing the step size, which turns out to leave the transitions essentially unaffected; the sharpness of the transitions remains within a step size of even an order of magnitude smaller than that applied in the current data.

C. Closure radius

The radius R_c at which the system closes can be predicted by requiring the packing density on the spherical surface to be (almost) the same as for a flat lattice, $R_c(N)=\sqrt{(N/4\pi)\cos(\pi/6)}$. For $N=6$, 25, 50, and 350 it follows that $R_c(N)=0.64$, 1.3, 1.9, and 4.9, respectively. These values agree with the data (Fig. 1 left) except for small N, where the packing is far less optimal than for a flat GEM lattice.

D. Structural transitions and topological defects

Energy jumps between different trajectories involve a major global rearrangement.

With successively applied small steps in curvature followed by relaxation, the system usually undergoes only minor local redistributions, while strain accumulates in parts of the lattice. At some curvature steps, however, an avalanche of sequential displacements over a major part of the system is triggered by local instabilities, while releasing much of the built-up strain. A small change in R may thus enforce a structural transition to a configuration, in which both the strain and the 2D topological (defect) structure have been drastically altered. An extensive systematic study of the topological defect structure as a function of N up to 200 is available.[6]

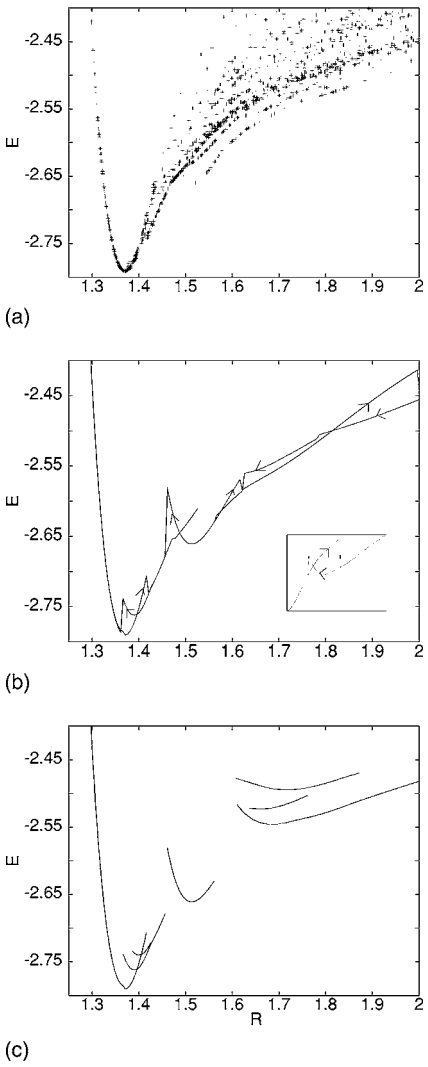

FIG. 2. Mean energy (E) vs curvature radius (R) for $N=25$. From top to bottom: (a) second experiment: energy minima at random fixed values of R, found in unbiased searches, each with random initial configuration, applying SA and SD; (b) third experiment: example of tracing through E-R space by 1% step in R using SD. The arrows indicate the R step direction. The inset shows a clear-cut case of hysteresis; (c) parts of trajectories exhibiting local minima as a function of R.

The transitions come along with incorporation or removal of defects as a function of curvature. Energy barriers are present between configurations with different topological structure. For the transition to take place requires the system to climb the barrier to a threshold before starting an avalanche of particle moves. The threshold R value depends on the barrier side, causing hysteresis.

Starting from an essentially circular patch with flat regular packing, the "unstable" radius R_u, where—with increasing curvature—the first structural transition occurs, is modeled as $S2n_{\max}\arcsin(\alpha)=\sin(2n_{\max}\arcsin(\alpha))$,[6] where $\alpha=1/(2R_u)$, $n_{\max}$ is essentially the largest completed hexagonal ring, and S can be taken from the data for a single specific N value (see Table I).

E. Open configurations

The points in Fig. 2(a) at large R cover a broad range in energy, corresponding to a great variety of open configurations and edge arrangements. As R decreases, the edge becomes smaller and the variation decreases. Any flexibility essentially disappears below R_c due to the strong constraints for a closed spherical configuration.

TABLE I. The radius R_u, where the trajectory becomes unstable for increasing curvature starting from a flat regular distribution for $N=6$, 50, 350, and 500, compared with the estimates from the simple model with S calibrated at $N=350$.

N	n (max)	R_u (data)	R_u (model)
6	1	1.37	1.34
50	3	3.95	4.11
350	9	12.3	12.3
500	11	15.6	15.0

F. Secondary minima

Fig. 2(b) shows E-R trajectories from the third experiment, starting from a specific configuration (near the minimum at $R\approx 1.5$) from the second experiment. Here the system is traced up and down in R. Indeed, the trajectories in the E-R plane connect unbiased solutions, and—like in the first experiment—jumps and the secondary minima occur. The secondary minima visible in Fig. 2(c), are obtained starting from the configurations of the second experiment [Fig. 2(c)], and tracing in R up and down until a jump occurs. The minima have a typical depth of 10% of the closure energy ΔE_c. At nonzero T the thermodynamic significance of such minima should be judged with respect to both kT and ΔE_c.

G. Variable *N*

The finding of distinct locally stable open configurations for fixed N raises the expectation that any discrete curvature may remain, or change smoothly, during growth when particles are added. A study of this type[15] indeed indicates that discrete locally stable configuration trajectories exist as a function of both R and N, where the bulk packing remains essentially the same.

V. CONCLUSION

In conclusion, for fixed N two-dimensional spherical Lennard-Jones systems at zero temperature, the global energy minimum with decreasing curvature radius R is approached through sharp transitions with major rearrangements. These transitions bring in topological defects connected with curvature. The curvature range of events relevant for self-assembly, R_u-R_c, is consistent with simple models. Apart from the closed (global) minimum energy configuration, secondary, local minima show up at larger R values, with an open configuration. This phenomenon—here shown for $N=25$—occurs naturally as a consequence of optimal packing topologies. During growth towards a complete shell such minima can capture "threads" of steady curvature along with growth in N, while staying in equilibrium. The present results and methods can help guide further generic studies of the self-organization in complex spherical molecular shells.

The authors are grateful to D. Frenkel (FOM-AMOLF) for many fruitful suggestions, and to M. Livny (UW-Madison) for indispensable support on Condor High Throughput Computing. Part of this work has been funded by the FOM and NWO science organizations in The Netherlands.

[1] W. S. Bont, Eur. J. Cell Biol. **39**, 458 (1985), and reference therein; see also http://arxiv.org/abs/cond-mat/0206343
[2] D. D. Lasic, *Liposomes: From Physics to Applications* (Elsevier, Amsterdam, 1993).
[3] S. Zhou, C. Burger, B. Chu *et al.*, Science **291**, 1944 (2001); J. Hao, H. Li, W. Liu, and A. Hirsch, Chem. Commun. (Cambridge) **2004**, 602.
[4] T. Liu, E. Diemann, H. Li, A. W. M. Dress, and A. Müller, Nature (London) **426**, 59 (2003).
[5] R. F. Bruinsma, W. M. Gelbart, D. Reguera, J. Rudnick, and R. Zandi, Phys. Rev. Lett. **90**, 248101 (2003).
[6] J. M. Voogd, Ph.D. thesis, University of Amsterdam, June 1998; www.science.uva.nl/research/scs/papers/jeroen.html
[7] M. Bowick, A. Cacciuto, D. R. Nelson, and A. Traesset, Phys. Rev. Lett. **89**, 185502 (2002); Phys. Rev. B **62**, 8738 (2000).
[8] J. Leech, Math. Gaz. **41**, 81–90 (1957).
[9] D. C. Rapaport, J. E. Johnson, and J. Skolnick, Comput. Phys. Commun. **121–122**, 231 (1999).
[10] See, for example, S. P. Giaritta, M. Ferrario, and P. V. Giaquinta, Physica A **201**, 649 (1993).
[11] J. A. Northby, J. Chem. Phys. **87**, 6166 (1987).
[12] C. J. Marzec and L. A. Day, Biophys. J. **65**, 2559 (1993).
[13] V. J. Reddy, P. Natarajan, B. Okerberg, K. Li, K. Damodaran, R. Morton, C. Brooks III, and J. E. Johnson, J. Virol. **75**, 11943 (2001).
[14] F. W. de Wette, R. E. Allen, D. S. Hughes, and A. Rahman, Phys. Lett. **A29**, 548 (1969).
[15] Reference 6, pp. 157 (to be published).
[16] T. Erber and G. M. Hockney, Phys. Rev. Lett. **74**, 1482 (1995); J. Phys. A **24**, 1369 (1991).
[17] P. J. M. van Laarhoven, and E. H. L. Aarts, *Simulated Annealing: Theory and Applications* (Kluwer Academic, Boston, MA, 1987), and references therein.
[18] D. J. Wales and J. P. K. Doye, J. Phys. Chem. A **101**, 5111 (1997) and reference therein.
[19] J. Moller, *Lecture Notes in Statistics Lectures on Random Voronoi Tessellations* (Springer, Berlin, 1994), Vol. 87.